

## OPTICAL AND ELECTRONIC PROPERTIES OF COAXIAL SQUARE QUANTUM WELL WIRES AND FIELD EFFECTS

Saban Aktas, Figen Karaca Boz, Sevket Erol Okan

*Department of Physics, Faculty of Science, Trakya University, 22030 Edirne, Turkey*

### Abstract

*The electronic and optical properties of the coaxial square quantum well wires were examined depending on their geometric parameters under external fields. Within the effective mass approximation, the finite difference and the variational methods were used in the calculations. The external fields such as electric, magnetic and laser fields affect the shape of the electronic wave function, and they also vary the energy states depending on their intensity. Thus, the blue shift in the total linear absorption coefficients can be provided as well as the photon energy.*

**Keywords:** Quantum well wire, energies, optical properties

### INTRODUCTION

Many studies have been devoted to semiconductor nanostructures which can be classified as quantum wells, quantum wires and quantum dots. They can be used in various electronic and photonic applications due to their rich physical properties [1-8]. Recently, advances in crystal growth techniques used for low-dimensional nanostructures have made it possible to obtain new arrangements of these structures with various semiconductor alloys and in various geometrical forms such as T-shaped, V-shaped, square and parabolic cross-sectioned shapes [9-12]. Additionally, research on multilayered quantum nanostructures is another direction. Mikhail and El Sayed [13] used different methods to calculate impurity states in spherical multilayer quantum dots. Karki et al. [14] reported barrier height effects in coaxial quantum wires under magnetic field. The effects of geometric size and magnetic field on coaxial cylindrical wires were investigated by Rezaei and Karimi [15]. Boz et al. [16] studied the geometric effects in a multilayer quantum dot with spherical cross-section under a magnetic field. Effects of electric field on impurity states in coaxial square *GaAs/AlGaAs* wire have been

presented by Aktaş et al. [17]. Kes et al. [18] reported the electronic properties of a coaxial QWW with an insulating layer under electric field. In recent years, research on the interaction of intense laser fields with electrons in semiconductors has increased with the emergence of high-power tunable laser sources. One of the such sources is free electron lasers (FEL). The effect of intense high-frequency laser field on physical properties in low-dimensional structures has been investigated in previous studies [19–22]. Again, in previous studies, it has been shown that the potential profiles of quantum structures intensely affect linear and non-linear absorption coefficients [23,24]. The effect of optical absorption coefficients on square quantum wires under laser field was investigated by Bekar et al. [24].

It is aimed to obtain the energy states and wave functions of an electron in square-section coaxial quantum wires, and to find the total linear absorption coefficients of all allowed transitions under external fields.

### THEORY

The structural view of the coaxial square quantum wires studied here is given in Fig.1. The system consists of two coaxial

equilateral square  $GaAs$  wires separated by a  $Al_{x_1}Ga_{1-x_1}As$  layer. The outer  $GaAs$  wire is also coated with a layer of  $Al_{x_2}Ga_{1-x_2}As$ . The  $Al_{x_1}Ga_{1-x_1}As$  layer creates a finite potential as the  $GaAs$  wires are connected allowing an electron to tunnel between them.

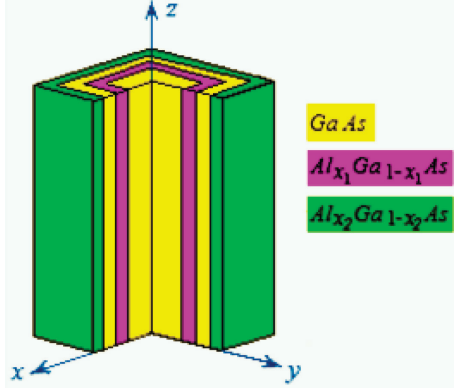


Fig. 1 The cross-sectional view of the coaxial wire

The Hamiltonian of an electron in the quantum wire system described in Fig.1, is given by under the magnetic field  $\vec{B}$  and electric field  $\vec{F}$  applied to the structure

$$H_0 = \frac{1}{2m^*c^2} [\vec{p}c + e\vec{A}]^2 + |e|Fx + V(x, y) \quad (1)$$

where  $m^*$  is the electron effective mass and  $e$  the elementary charge. Magnetic vector potential gauge  $\vec{A}$  was chosen

$$\vec{A} = \left( -\frac{1}{2}B_y\hat{x}, \frac{1}{2}B_x\hat{y} \right) \quad , \quad (2)$$

and  $V(x, y)$  the finite confining potential for electron given by

$$V(x, y) = \begin{cases} 0, & 0 \leq x < 0.5a^* \text{ and } 0 \leq y < 0.5a^* \\ V_0, & 0.5 \leq x < 1.0a^* \text{ and } 0.5 \leq y < 1.0a^* \\ 0, & 1.0 \leq x < 1.5a^* \text{ and } 1.0 \leq y < 1.5a^* \\ V_0, & 1.5 \leq x < \infty \text{ and } 1.5 \leq y < \infty \end{cases} \quad (3)$$

If one use  $a^* = \hbar^2\epsilon/m^*e^2$  and  $R^* = m^*e^4/2\hbar^2\epsilon^2$  as the units of reduced length and energy, respectively, while laser field vector potential is to be

$$\vec{A} = A_0 \cos(\omega_d t) \hat{x} \quad , \quad (4)$$

and for  $\vec{p} = -i\hbar\vec{\nabla}$ , the Hamiltonian in Eq.1 can be expressed in the form of

$$H_0 = -\nabla^2 + \eta x + \gamma^2 \frac{(x^2 + y^2)}{4} + V_{DC}(x, y) \quad , \quad (5)$$

where  $\gamma = e\hbar B(2m^*cR^*)^{-1}$ ,  $\eta = |e|a^*F(R^*)^{-1}$ , and

$$V_{DC}(x, y) \cong \frac{\omega_d}{2\pi} \int_0^{2\pi/\omega_d} V(x, y, t) dt \cong \frac{1}{2\pi} \int_0^{2\pi} V(x + \alpha_0 \sin\varphi, y) d\varphi \quad . \quad (6)$$

Then, the wavefunctions  $\Psi_n(x, y)$  and energy levels  $E_n$  of the electron can be found from the Schrödinger equation

$$H_0\Psi_n(x, y) = E_n\Psi_n(x, y) \quad . \quad (7)$$

All energies and wavefunctions were calculated by the finite differences method.

The linear optical absorption coefficient is

$$\beta(\omega) = \hbar\omega \sqrt{\frac{\mu}{n_s^2\epsilon_0}} \left[ \frac{\sigma |M_{if}|^2 \tau_{if}^{-1}}{(E_{if} - \hbar\omega)^2 + \hbar^2 \tau_{if}^{-2}} \right] \quad . \quad (8)$$

The dipol matrix element  $M_{if}$  in Eq.7 is given by

$$M_{if} = e \int_{-\infty}^{+\infty} \int_{-\infty}^{+\infty} \Psi_i(x, y) x \Psi_f(x, y) dx dy \quad . \quad (9)$$

## RESULTS

The electronic and optical properties of the coaxial square quantum well wire structure were obtained under the electric, magnetic, and laser fields. The Rydberg energy and effective Bohr Radius were used as  $R^* = 5.83 \text{ meV}$ , and  $a^* = 100 \text{ \AA}$ , respectively. The structural constants are  $V_0 = 41 R^*$ , the electron density  $\sigma = 3 \times 10^{22} \text{ m}^{-3}$ , the refractive index  $n_s = 3.2$ , the relaxation coefficient  $\tau_{if} = 0.2 \text{ ps}$ , and the optical intensity  $I = 0.3 \text{ MW/cm}^2$ .

In Fig. 2, the first ten electronic energy levels are shown as functions of electric field intensity. The background energy  $E_1$  follows a constant course until the electric field increases to  $\sim 12 \text{ kV/cm}$ , then it shows a linear decrease with increasing intensity for fields larger than this threshold intensity. The energy states  $E_2$  and  $E_3$  exhibit a crossing at an electric field strength of  $\sim 15 \text{ kV/cm}$ . Another crossing is also observed between the energy states  $E_9$  and  $E_{10}$  at  $\sim 16 \text{ kV/cm}$ . The  $E_7$  and  $E_8$  are degenerate until the electric field intensity increased up to  $10 \text{ kV/cm}$ .

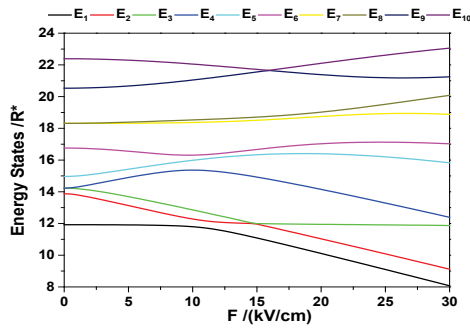


Fig.2 Electric field effect on first ten energy states.

Another interesting point in Fig.2 is that, the energy states  $E_3$  and  $E_4$  are degenerate, and the  $E_2$  is very close to these two energy levels when there is no electric field. Fig.3 presents the wave function of an electron in the  $E_2$  level in three dimensions when no external field is applied for that case. The wave function exhibits a symmetrical distribution mostly localizing on the outer corners of the structure. Fig. 4 compares the wave functions of the electron in the degenerate  $E_3$  and  $E_4$  as in-plane contour plots. These wave functions, which are essentially identical, but have  $90^\circ$  of rotational symmetry with respect to each other.

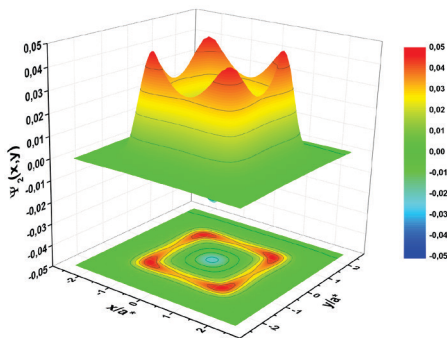


Fig.3 The three dimensional representation of electronic wavefunction at second energy level.

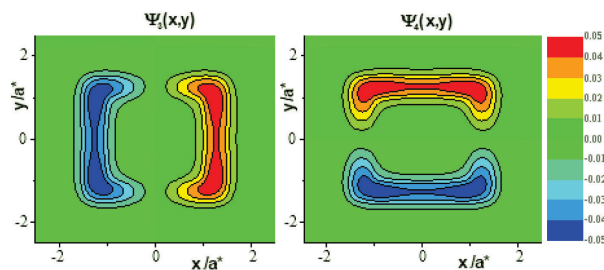


Fig.4 The two dimensional footprints of electronic wavefunctions at third (the left-hand side) and fourth (the right-hand side figure) energy levels.

Application of a magnetic field, like electric field, is another probe that characterizes the electronic and optical properties of low-dimensional structures. The change of energy states of the structure consisting of coaxial quantum wires modelled here depending on the applied magnetic field intensity is reflected in Fig. 5. The  $E_1$  energy state follows an almost constant value course with increasing magnetic field intensity compared to other energy states. The degeneracy of  $E_3$  and  $E_4$  energy levels come across in no-field is applied becomes permanent, this time up to a value of approximately  $1.7 T$ . In addition, in the structure with a potential depth of  $V_0 = 41 R^*$ , at high magnetic field intensities, all excited energy levels, especially  $E_{10}$ , climb towards this depth value. Another interesting point is that, as a general trend, energy states that increase exponentially with the magnetic field show a plateau in the high mid-range intensities.

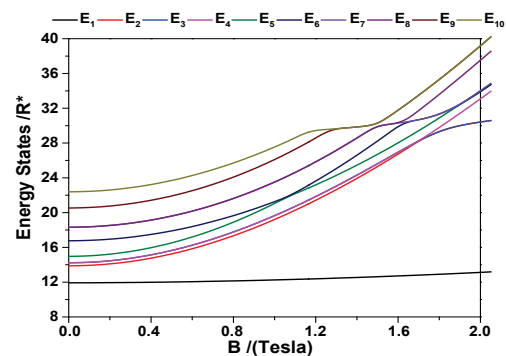


Fig.5 Magnetic field effect on first ten energy states.

Apparently, potential profiles of low dimensional structures can be altered and controlled, and so their electronic and optical properties, by laser fields [19-22]. With this motivation, the electronic properties of the structure targeted to be examined are shown in Fig. 6 as functions of laser field intensity in addition to the electric and magnetic field applications. This time, while  $E_1$  shows a curvilinear behavior with a minimum with increasing laser field intensity, it becomes degenerate with  $E_2$  in areas larger than  $0.4 a^*$ . Depending on the increasing laser field intensity, in the energy states from  $E_8$  to  $E_{10}$ , a tendency to exceed the  $V_0 = 41 R^*$  depth with a rapid climb, that is, to release

the electron from where it is confined, is observed.

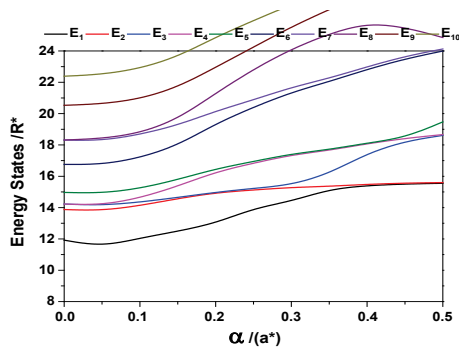


Fig.6 Laser field effect on first ten energy states.

Optical properties are discussed in this study on the basis of calculating linear absorption coefficients as functions of photon energy. The total linear absorption coefficient in the coaxial wires without electric field and with 10 *kV/cm* and 20 *kV/cm* field strengths are shown in Fig.7. The total linear absorption coefficient means the addition of all possible transitions. It is observed that in the absence of an electric field, all transitions occur with three peaks in the 0 – 35 *meV* photon energy range. For the 10 *kV/cm* field strength application, the number of peaks decreases by two, while a small shift towards higher photon energies is observed. For a field strength of 20 *kV/cm*, the three peak appearance returns and the photon energy range increases to 0 – 75 *meV*. The total absorption coefficient was also calculated under 0.25 *a\** and 0.5 *a\** laser fields. However, the results are not given here for the sake of brevity because they were very similar to those obtained for 10 *kV/cm* and 20 *kV/cm* electric field strengths.

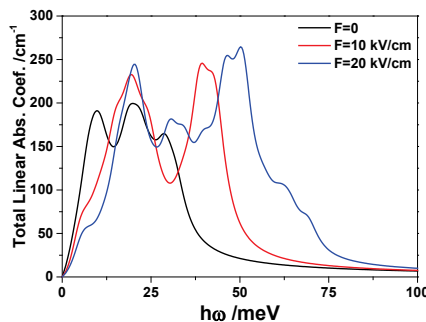


Fig.7 The linear absorption coefficients in the coaxial wires without electric field and with 10 and 20 *kV/cm* field strengths.

The results shown in Fig.8 show the behavior of the total linear absorption coefficient under two different magnetic field intensities. For *B* = 1 *Tesla*, the energy range in which all transitions expands to 0 – 70 *meV* range, while the coefficient shows a slight increase compared to its no-field values.

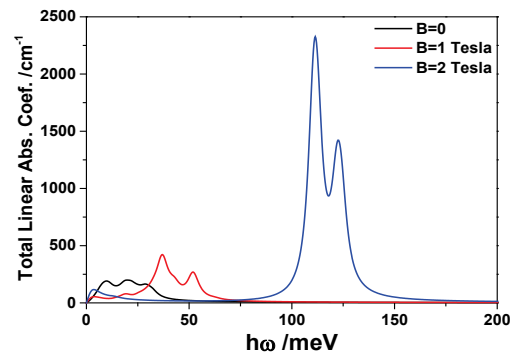


Fig.8 The linear absorption coefficients in the coaxial wires without magnetic field and with 1 and 2 *Tesla* field strengths.

For *B* = 2 *Tesla*, two well-defined peaks in the narrow 100 – 150 *meV* range are observed and the photon energy range occurs with a large increase. Meanwhile, the application of 2 *Tesla* increases the absorption coefficient approximately seven to ten times compared to its magnitudes at no-field and 1 *Tesla* field strength.

## CONCLUSION

The electronic and optical properties of the coaxial quantum well wire, which has a symmetrical structure, were determined depending on the variations in the energy states due to externally applied electric, magnetic and laser fields. The material composition of the wire was chosen to be *GaAs/Al<sub>x</sub>Ga<sub>1-x</sub>As*. It was observed that external fields applied to the structure created significant characteristic changes in the energy states depending on their intensity. In particular, high magnetic field intensities can increase the total linear absorption coefficient maxima by up to 10 fold compared to those obtained at low magnetic field intensities.



## REFERENCES

- [1] Bati M. The effects of the intense laser field on the resonant tunneling properties of the symmetric triple inverse parabolic barrier double well structure. *Physica B: Physics of Condensed Matter*. 2020; 594: 412314.
- [2] Boz F.K., Nisanci B., Aktas S., Okan S.E. Energy levels of GaAs/Al<sub>x</sub>Ga<sub>1-x</sub>As/AlAs spherical quantum dot with an impurity. *Applied Surface Science*. 2016; 387: 76.
- [3] Turkoglu A., Dakhlaoui H., Mora-Ramos M.E., Urgan F. Optical properties of a quantum well with Razavy confinement potential: role of applied external fields. *Phys. E Low-Dimensional Syst. Nanostruct.* 2021; 134: 114919.
- [4] Bera A., Ghosh A., Arif S.M., Ghosh M. Exploring quadrupole oscillator strength of impurity doped quantum dots controlled by Gaussian white noise. *European Physical Journal D*. 2020;74: 230.
- [5] Sedehi H.R.R., Khordad R., Bahramiyan H. Optical properties and diamagnetic susceptibility of a hexagonal quantum dot: impurity effect. *Optical and Quantum Electronics*. 2021;53: 264.
- [6] Gulyamov G., Gulyamov A.G., Davlatov A.B., Juraev K.N. Energy Levels in Nanowires and Nanorods with a Finite Potential Well. *Advances in Condensed Matter Physics*. 2020; 4945080.
- [7] Bekar B., Boz F. K., Aktas S., Okan S. E. The Effect on the Optical Absorption Coefficients due to the Positions in the Plane of Square GaAs / Al(GaAs) Quantum Well Wire under the Laser Field. *Acta Physica Polonica A*. 2019;136: 882-888.
- [8] You JH., Guo KX. Effect of terahertz laser field on anisotropic optical absorption and refractive index changes of coaxial square quantum well wires. *Physica B*. 2021; 615: 413085.
- [9] Jensen J.R., Hvam J.M., Langbein W. Enhanced confinement energy in strained asymmetric T-shaped quantum wires. *Journal of Crystal Growth*. 2001; 227-228: 966-969.
- [10] Giraldo-Tobon E., Ospina W., Miranda G.L., Fulla M.R. Energy spectrum analysis of a realistic single-electron Ga<sub>1-x</sub>Al<sub>x</sub>As/GaAs/Ga<sub>1-x</sub>Al<sub>x</sub>As quantum V-groove in external electric field. *Physica E: Low-dimensional Systems and Nanostructures*. 2019; 114: 113652.
- [11] Rezaei G., Mousavi S., Sadeghi E. External electric field and hydrostatic pressure effects on the binding energy and self-polarization of an off-center hydrogenic impurity confined in a GaAs/AlGaAs square quantum well wire. *Physica B*. 2012; 407: 2637-2641.
- [12] An XT., Liu JJ. Hydrogenic impurities in parabolic quantum-well wires in a magnetic field. *Journal of Applied Physics*. 2006; 99: 12.
- [13] Mikhail I.F.I., El Sayed S.B.A. Exact and variational calculations of a hydrogenic impurity binding energy in a multilayered spherical quantum dot. *Physica E*. 2011; 43: 1371-1378.
- [14] Karki H.D., Elagöz S., Baser P., Amca R., Sokmen I. Barrier height effect on binding energies of shallow hydrogenic impurities in coaxial GaAs/ Al<sub>x</sub>Ga<sub>1-x</sub>As quantum well wires under a uniform magnetic field. *Superlattices and Microstructures*. 2007; 41: 227-236.
- [15] Rezaei G., Karimi M. J., Third harmonic generation in a coaxial cylindrical quantum well wire: Magnetic field and geometrical size effects. *Optics Communications*. 2012; 285: 5467-5471.
- [16] Boz F. K., Aktas S., Bilekkaya A., Okan S. E. The multilayered spherical quantum dot under a magnetic field. *Applied Surface Science*. 2010; 256: 3832-3836.
- [17] Aktas S., Boz F. K., Bilekkaya A., Okan S. E. The electronic properties of a coaxial square GaAs/Al<sub>x</sub>Ga<sub>1-x</sub>As quantum well wire in an electric field. *Physica E*. 2009; 41: 1572-1576.
- [18] H. Kes, A. Bilekkaya, S. Aktas, S. E. Okan Binding energy of a hydrogenic impurity in a coaxial quantum wire with an insulator layer. *Superlattices and Microstructures*. 2017; 111: 966-975.
- [19] Boz F.K., Aktas S., Bekar B., Okan S.E., Laser field-driven potential profiles of double quantum wells. *Phys. Lett. A*. 2012; 376: 590.
- [20] Lima F.M.S., Amato M.A., Nunes O.A.C., Fonseca A.L.A., Enders B.G., da Silva E.F. Unexpected transition from single to double quantum well potential induced by intense laser fields in a semiconductor quantum well. *J. Appl. Phys.* 2009; 105: 123111.

[21] Zhang C. Resonant tunneling and bistability in a double barrier structure under an intense terahertz laser. Appl. Phys. Lett. 2001; 78: 4187.

[22] Ozturk E., Sokmen I. Nonlinear Intersubband Transitions in Square and Graded Quantum Wells Modulated by Intense Laser Field. Chin. Phys. Lett. 2014; 31: 127301.

[23] Kasapoglu E., Duque C.A., Sari H., Sökmen I. Intense laser field effects on the linear and

nonlinear intersubband optical properties of a semi-parabolic quantum well. Eur. Phys. J. B. 2011; 82: 13.

[24] Bekar B., Boz F.K., Aktas S., Okan S.E. The Effect on the Optical Absorption Coefficients due to the Positions in the Plane of Square GaAs / Al(GaAs) Quantum Well Wire under the Laser Field. Acta Physica Polonica A. 2019; 136: 882.